Pis'ma v ZhETF, vol. 100, iss. 1, pp. 47 – 58

Transient and steady-state properties of asymmetric semiconductor quantum wells at Telecom wavelength bands

H. R. Hamedi[1)]

Institute of Theoretical Physics and Astronomy, Vilnius University, LT-01108 Vilnius, Lithuania

Submitted 14 April 2014
Resubmitted 2 June 2014

Transient and steady-state dispersion and absorption properties of a three-subband asymmetric semiconductor quantum well system are investigated. In the steady-state regime, it is shown that by increasing the strength of Fano-interference as well as enhancement of energy splitting of two excited states the slope of dispersion changes from negative to positive which is corresponding to a switch between superluminal to subluminal light propagation. At the same time, the probe absorption reduces at telecommunication wavelength $\lambda = 1550\,\text{nm}$. The influence of incoherent pumping fields on time-dependent susceptibility is then discussed. It is found that due to more transfer of population to the upper levels, increasing the rate of incoherent pump field leads to the reduction of probe absorption. In addition, it is realized that incoherent pumping has a major role in converting fast to slow propagation of light at long wavelength. We also introduce an extra controllability for the light pulse to be slow downed at Telecom wavelength just through the quantum interference arising from incoherent pumping fields. The obtained results may be practical in telecommunication applications.

DOI: 10.7868/S0370274X14130098

1. Introduction. The propagation of light pulse through a dispersive medium has been recently investigated [1–4]. Superluminal light propagation is a phenomenon in that group velocity an optical pulse in a dispersive medium is greater than of the light in vacuum. It is shown that by modifying the coherence of the light pulse, the propagation changes from superluminal to subluminal [5]. It is well known that the quantum coherence and interference are important mechanisms to modify the optical properties of the light pulse [6–9]. The absorption pulse propagation of a weak probe beam in a two level atom driven by an intense field have been studied by Mallow [10]. Harris [11] shows that electromagnetically induced transparency (EIT) [12, 13] can cancel the absorption in the medium. Recently, absorption and dispersion properties of a weak probe field have attracted considerable attention, because they can lead to superluminal and subluminal light propagation. Absorption free superluminal light propagation in a three-level pumped-probe system has also been examined [14]. Due to normal applications, realization of an absorption two photon optical switch for instance, the four-level EIT medium have widely been investigated to observe subluminal and superluminal light propagation [15, 16]. In one of our recent studies, the absorption-dispersion properties of a four level Lambda type atomic system was investigated [17]. It is found that the slope of dispersion not only changes by the intensity of coupling field, but also it changes by the rate of an incoherent pump field. It is worth noting that one can study the optical properties of a semiconductor quantum well [18–21]. The reason for this is mainly that the phenomena in the SQWs have many potentially important applications in optoelectronics and solid-state quantum information science. Otherwise, devices based on intersubband transitions in the SQWs have many inherent advantages that the atomic systems do not have, such as the large electric dipole moments due to the small effective electron mass, the great flexibilities in devices design by choosing the materials and structure dimensions, the high nonlinear optical coefficients, and the transition energies and the dipoles as well as the symmetries can also be engineered as desired.

In this work, we intend to study the absorption and dispersion of the probe field in a three-level asymmetric semiconductor quantum well system. We discuss the steady-state behaviour of the system and demonstrate that the probe dispersion and absorption can be controlled by the strength of Fano-interference and energy splitting of two excited states. Then, choosing a transient regime, we study the dependence of optical properties of QW sample on the rate of incoherent pumping.

2. Model and equations. The semiconductor double QW structure consisting of two quantum wells that

[1)]e-mail: Hamid.R.Hamedi@gmail.com

are separated by a narrow barrier is shown in Fig. 1 [22, 23]. The $|a\rangle$ and $|b\rangle$ are the first subband of the

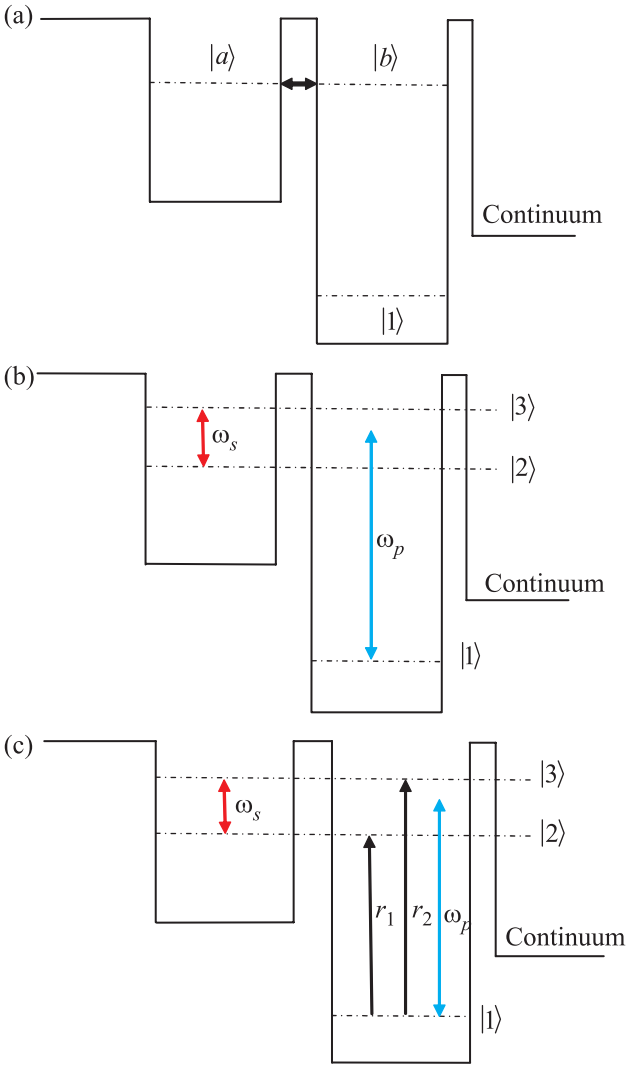

Fig. 1. (a) – Energy level diagram of a double quantum well structure. It consists of two quantum wells and a collector region separated by thin tunnelling barriers. (b) – Due to the strong coherent coupling via the thin barrier, the levels split into a doublet $|2\rangle$ and $|3\rangle$, which are coupled to a continuum by a thin tunnelling barrier adjacent to the deep well. ω_s denotes the splitting between the two upper levels (given by the coherent coupling strength) and ω_p is the weak probe laser. (c) – Schematic diagram of the quantum well system applied by two incoherent pumping r_1 and r_2

shallow well and the second subband of the deep well, respectively, which are resonant (see Fig. 1a). Due to the strong coherent coupling via the thin barrier, the levels split into a doublet levels $|2\rangle$ and $|3\rangle$, which arise from the mixing of the states $|a\rangle$ and $|b\rangle$, under the exactly resonant conditions, $|2\rangle = (|a\rangle - |b\rangle)/\sqrt{2}$, $|3\rangle = (|a\rangle + |b\rangle)/\sqrt{2}$. The splitting energy ω on resonance is given by the coupling strength and can be controlled by adjusting the height and width of the tunnelling barrier with applied bias voltage [24]. A low intensity pulsed laser field ω_p (amplitude E_p) is applied to the transitions $|1\rangle \to |3\rangle$ and $|1\rangle \to |2\rangle$ simultaneously with the respective Rabi frequencies $\Omega_{p_1} = \mu_{31}E_p/2\hbar$ and $\Omega_{p_2} = \mu_{21}E_p/2\hbar$ with μ_{31} and μ_{21}, and being the intersubband dipole moments of the respective transition. The small signal absorption of the weak-probe field propagating through such a system can be computed in the steady state.

In the interaction representation and under the rotating-wave approximations, the semi-classical Hamiltonian describing the interaction for the system under study is given by ($\hbar = 1$)

$$H_{\rm int} = \Delta_p(|2\rangle\langle 2| + |3\rangle\langle 3|) - \Omega_p(|2\rangle\langle 1| + |3\rangle\langle 1| + \text{h.c.}). \quad (1)$$

Where the probe laser detuning is defined as $\Delta_p = \omega_0 - \omega_p$, while the average transition frequency is denoted by $\omega_0 = (\omega_2 + \omega_3)/2$.

By adopting the standard approach [25–28], we can easily obtain the density-matrix equations of motion in electro-dipole and rotating-wave approximations as follows:

$$\dot\rho_{12} = -\frac{\gamma_{21}}{2}\rho_{12} + i\left(\Delta_p - \frac{\omega_s}{2}\right)\rho_{12} + i\Omega_{p_2}(\rho_{22} - \rho_{11}) + i\Omega_{p_1}\rho_{32} - \frac{\eta}{2}\rho_{13},$$

$$\dot\rho_{13} = -\frac{\gamma_{31}}{2}\rho_{13} + i\left(\Delta_p + \frac{\omega_s}{2}\right)\rho_{13} + i\Omega_{p_1}(\rho_{33} - \rho_{11}) + i\Omega_{p_2}\rho_{23} - \frac{\eta}{2}\rho_{12},$$

$$\dot\rho_{23} = -\frac{\gamma_{32}}{2}\rho_{23} + i\omega_s\rho_{23} + i\Omega_{p_2}\rho_{13} - i\Omega_{p_1}\rho_{21} - \frac{\eta}{2}(\rho_{22} + \rho_{33}),$$

$$\dot\rho_{22} = -\gamma_2\rho_{22} + i\Omega_{p_2}(\rho_{12} - \rho_{21}) - \frac{\eta}{2}(\rho_{23} + \rho_{32}),$$

$$\dot\rho_{33} = -\gamma_3\rho_{33} + i\Omega_{p_1}(\rho_{13} - \rho_{31}) - \frac{\eta}{2}(\rho_{23} + \rho_{32}),$$

$$\rho_{11} + \rho_{22} + \rho_{33} = 1. \quad (2)$$

Here $\omega_s = E_3 - E_2$ is the energy splitting between the upper levels, given by the coherent coupling strength of the tunnelling. The population decay rates and dephasing decay rates are added phenomenologically in the above equations [28]. The population decay rates for subband $|i\rangle$, denoted by γ_i, are due primarily to longitudinal optical (LO) phonon emission events at low temperature. The total decay rates γ_{ij} $(i \neq j)$ are given by $\gamma_{21} = \gamma_2 + \gamma_{21}^{\rm dph}$, $\gamma_{31} = \gamma_3 + \gamma_{31}^{\rm dph}$, and $\gamma_{32} = \gamma_2 + \gamma_3 + \gamma_{32}^{\rm dph}$, where $\gamma_{ij}^{\rm dph}$ determined by electron-electron, interface

roughness, and phonon scattering processes, is the dephasing decay rate of the quantum coherence of the $|i\rangle \rightarrow |j\rangle$ transition. The parameter $\eta = \sqrt{\gamma_2\gamma_3}$ represents cross coupling between the states $|2\rangle$ and $|3\rangle$ via the LO phonon decay, it describes the process in which a phonon is emitted by subband $|2\rangle$ and is recaptured by subband $|3\rangle$. These mutual coupling terms can be obtained if tunnelling is present, e.g., through an additional barrier next to the deeper well [24, 30]. As mentioned above, levels $|2\rangle$ and $|3\rangle$ are both the superpositions of the resonant states $|a\rangle$ and $|b\rangle$. Because the subband $|b\rangle$ is strongly coupled to a continuum via a thin barrier, the decay from state $|b\rangle$ to the continuum inevitably results in these two dependent decay pathways: from the excited doublet to the common continuum. That is to say, the two decay pathways are related: the decay from one of the excited doublets can strongly affect the neighbouring transition, resulting in the interference characterized by those mutual coupling terms. The probe absorption can be controlled due to the Fano interference between the two decay paths. Such interference is similar to the "decay-induced" coherence in atomic systems with two closely lying energy states and occurs due to quantum interference in the electronic continuum [24]. The intensity of the Fano interference [24, 31], defined by $p = \eta/\sqrt{\gamma_{21}\gamma_{31}}$, and the values $p = 0$ and 1 correspond to no interference (there is no negligible coupling between levels $|2\rangle$ and $|3\rangle$, this means that Fano-interference does not generate) and perfect interference (no dephasing decay rates $\gamma_{ij}^{\rm dph} = 0$), respectively. It is worth noting that the above described parameter p is mainly controlled via the population decay rates $\gamma_i(\gamma_1, \gamma_2)$ and dephasing decay rates $\gamma_{ij}^{\rm dph}$, and it appears when the cross coupling term is present ($\eta \neq 0$), but disappears when the cross coupling term is absent ($\eta = 0$).

Equations (1) can be solved to obtain the steady state response of the medium. The linear susceptibility can be written as:

$$\chi = \frac{2N}{\varepsilon_0\hbar\Omega_p}(\mu_{21}^2\rho_{21} + \mu_{31}^2\rho_{31}). \qquad (3)$$

For further discussion in linear optical properties of the medium, we introduce the group index $n_g = c/\nu_g$, where c is the speed of light in vacuum and the group velocity is given by [32–34]:

$$\nu_g = \frac{c}{1 + 2\pi\chi' + 2\pi\nu_g\partial\chi'/\partial\nu_g}, \qquad (4)$$

where ν_g is the frequency of the probe field. The linear susceptibility χ is a complex quantity that is defined as $\chi = \chi' + i\chi''$.

3. Results and discussion. With the initial conditions $\rho_{11}(0) = 1$ and the other $\rho_{ij}(0)$ $(i, j = 1, 2, 3)$, we begin with investigating the steady-state and transient response of susceptibility by solving the time-dependent density matrix Eqs. (2) numerically via some nice MATLAB codes. For the steady-state regime, the set of Eqs. (2) can be written in the form of one deferential matrix equation: $\dot{R} = -MR + C$, where R and C are column vectors and M is the matrix of coefficients. The formal solution of such an equation is given by: $R(t) = \int_{-\infty}^{t} e^{-M(t-t')}Cdt' = M^{-1}C$. In addition, for the transient regime, we used four-order Rang-kutta method to plot the dynamical behavior of susceptibility and population distribution.

3.1. The case in absence of incoherent pumping; steady-state regime. It is well known that the group velocity of a probe field strongly depends on the slope of dispersion (the real part of the susceptibility). We show that the slope of dispersion can be changed from negative to positive or vice versa by the quantum interference induced by Fano-interference mechanism. In addition, the effect of energy splitting upon the probe absorption and dispersion are discussed. Thus, the strength of Fano-interference change the linear susceptibility leading to change of group velocity from superluminal to subluminal light propagation. Now, we present the results in Figs. 2–5. We consider $\gamma_2 = 5.6\gamma$ and $\gamma_3 = 7\gamma$ and all the parameters are reduced to the dimensionless units though scaling by γ. Moreover, we choose $\mu_{21} = \mu_{31} = \mu$, $\Omega_{p_1} = \Omega_{p_2} = \Omega_p$ and all the figures are normalized by $2N\mu/\varepsilon_0\hbar\Omega_p = 1$.

First, the effect of quality or strength of the Fano-type interference on linear susceptibility as well as group velocity is displayed in Fig. 2. It can be realized from Fig. 2a that for a fixed energy splitting, i.e., $\omega_s = 5\gamma$ and the small strength of the Fano-interference, i.e., $p = 0.46$, the slope of dispersion is negative at $\lambda = 1550\,\text{nm}$, which is accompanied with an absorption peak. The corresponding group indexes $(c/\nu_g - 1)$ is shown in Fig. 2b. It is observed that a superluminal group velocity propagates through the medium with a large absorption. Investigation on Fig. 2c shows that by increasing the strength of the Fano interference from $p = 0.46$ to 0.63 the slope of the dispersion changes from negative to positive and thus, the group velocity changes from superluminal to subluminal as can be seen from Fig. 2d. In this case, the absorption line-shape exhibits a dip around $\lambda = 1.55 \cdot 10^{-6}\,\text{m}$. Investigation on Fig. 2e shows that for an strong strength of Fano-interference i.e. $p = 0.77$ the probe absorption is substantially decreased with respect to Figs. 2a and c. Within this narrow reduced

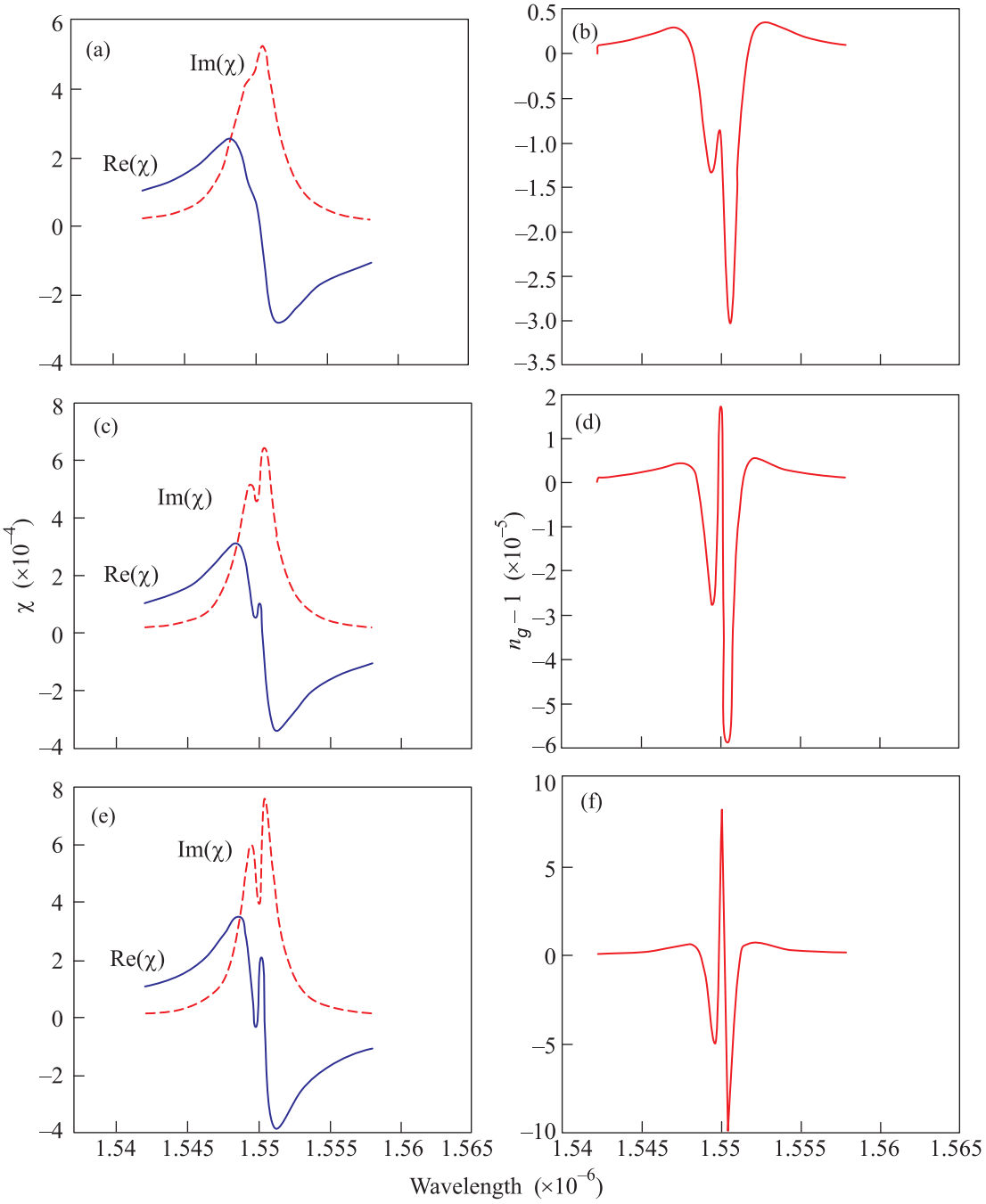

Fig. 2. Real and imaginary parts of the linear susceptibility (a, c, e), and group index (b, d, f) versus probe field wavelength for different strength of the Fano-interference. The selected parameters are ($p = 0.46$): $\gamma_{21}^{\rm dph} = 6\gamma$, $\gamma_{31}^{\rm dph} = 9.2\gamma$, $\gamma_{32}^{\rm dph} = 7.6\gamma$ (a, b); ($p = 0.63$): $\gamma_{21}^{\rm dph} = 3\gamma$, $\gamma_{31}^{\rm dph} = 4.6\gamma$, $\gamma_{32}^{\rm dph} = 3.8\gamma$ (c, d); ($p = 0.77$): $\gamma_{21}^{\rm dph} = 1.5\gamma$, $\gamma_{31}^{\rm dph} = 2.3\gamma$, $\gamma_{32}^{\rm dph} = 1.9\gamma$ (e, f). The other parameters are $\omega_s = 5\gamma$, $\gamma_2 = 5.6\gamma$, $\gamma_3 = 7\gamma$, $\Omega_p = 0.001\gamma$

absorption region the slope of dispersion is very steep which suggests a subluminal light propagation (Fig. 2f) via strength of Fano-interference mechanism. Physically, the quantum interference parameter η remains fixed when $\gamma_2 = 5.6\gamma$ and $\gamma_3 = 7\gamma$, but the varying dephasing rates $\gamma_{ij}^{\rm dph}$ influence the strength of the Fano-interference p, which affects the probe absorption and dispersion.

Figs. 3–5 show the probe absorption-dispersion versus probe field wavelength for different values of the energy splitting ω_s. It can be realized from Fig. 3a that for the small strength of the Fano-interference, i.e., $p = 0.46$

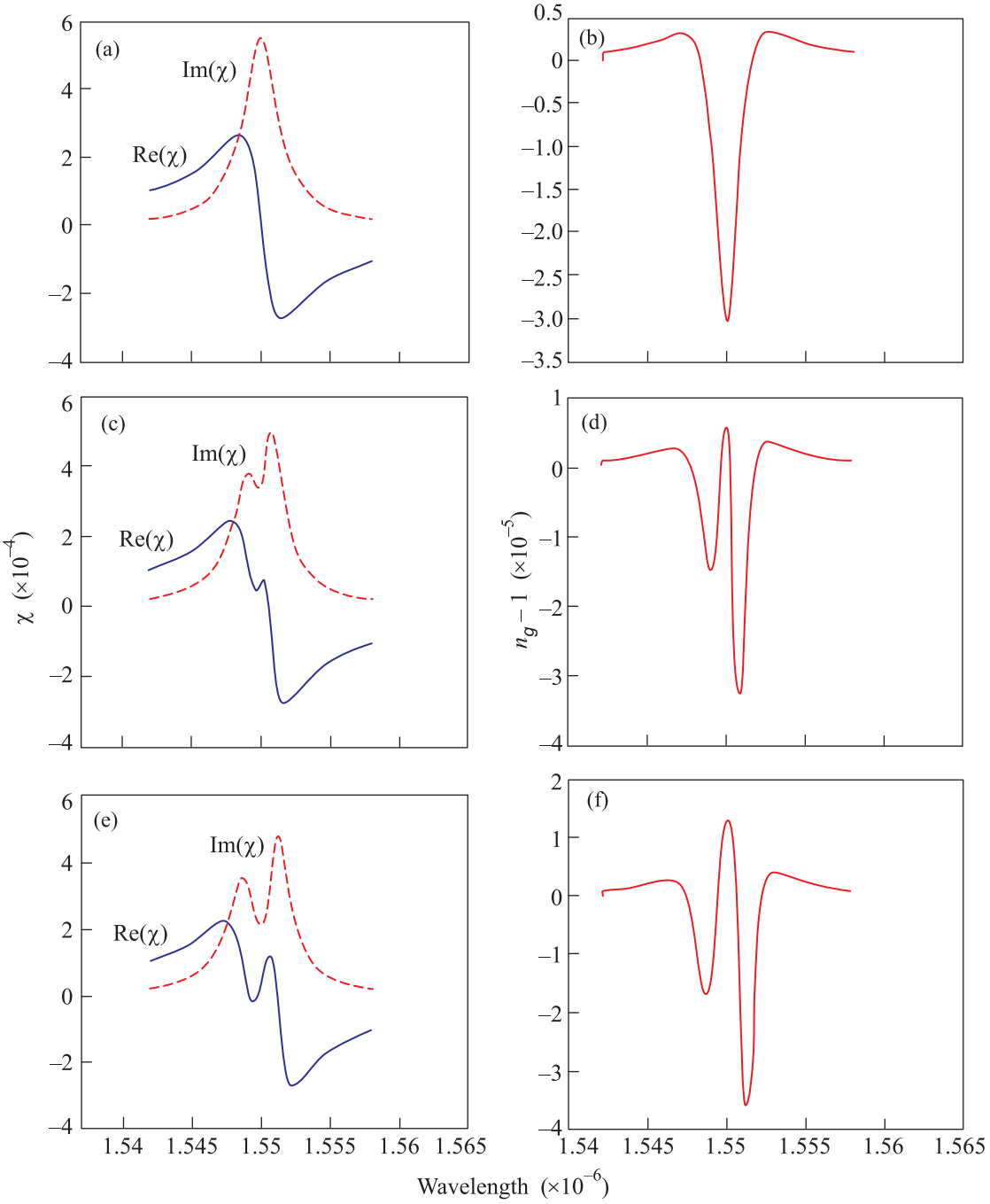

Fig. 3. Real and imaginary parts of the linear susceptibility (a, c, e), and group index (b, d, f) versus probe field wavelength for different energy splitting ω_s. The parameters are $p = 0.46$ and $\omega_s = 0.5\gamma$ (a, b), 9γ (c, d), 15γ (e, f). The other parameters are the same as Fig. 2

and for $\omega_s = 0.5\gamma$, the medium experiences a large absorption around long wavelength $\lambda = 1550\,\text{nm}$ and the phenomenon is called EIA [35–38]. For such a case the slope of the dispersion becomes negative and superluminal light propagation occurs (Fig. 3b). Investigation on Figs. 3c and e shows that increasing the energy splitting to $\omega_s = 9\gamma$ and 15γ can reduce the probe absorption around $\lambda = 1.55 \cdot 10^{-6}\,\text{m}$. In this case, the slope of dispersion switches to positive which is corresponding to subluminal light propagation. The curves for group indexes in these cases are displayed in Figs. 3d and f. The similar curves are displayed for $p = 0.63$ and for given

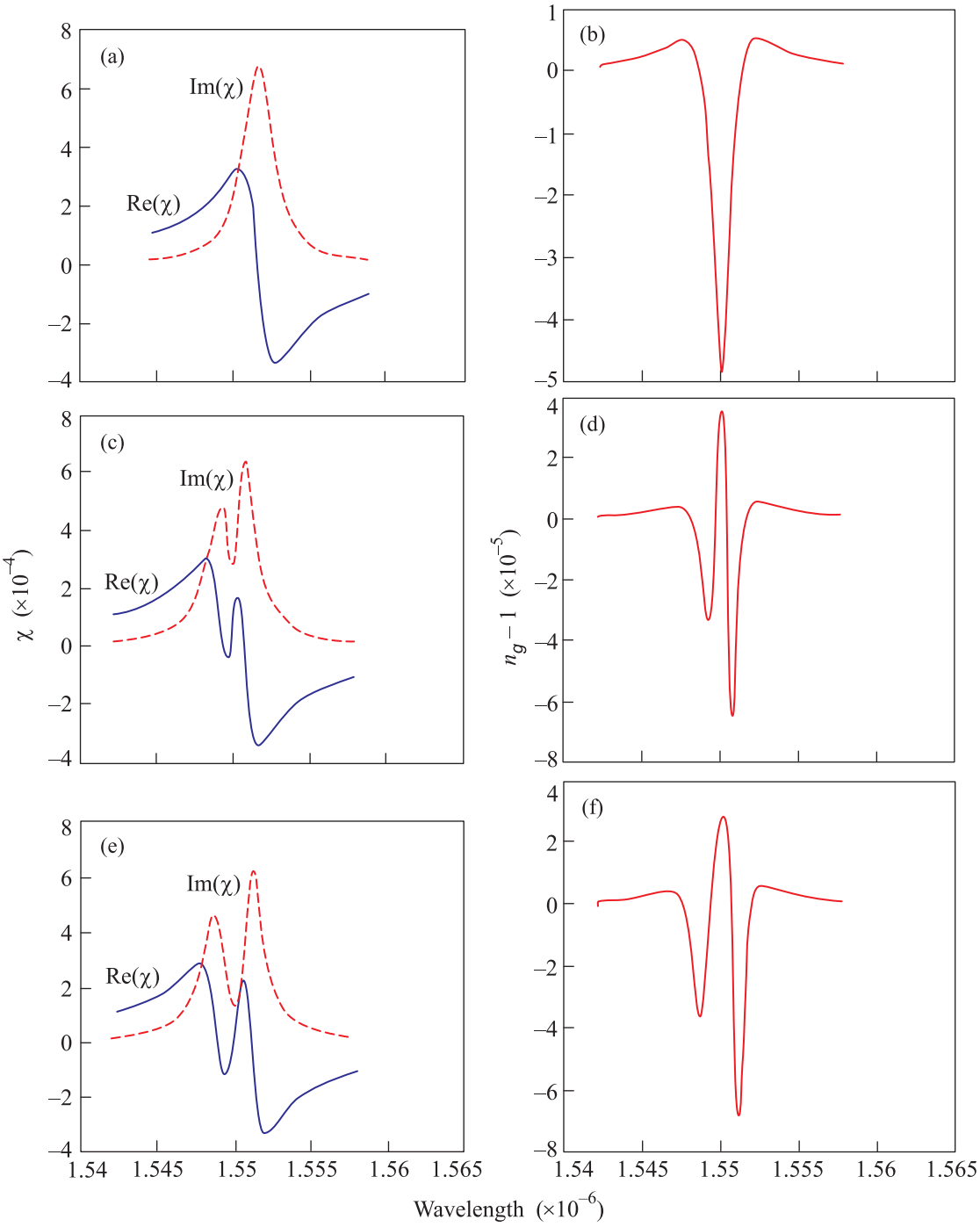

Fig. 4. Real and imaginary parts of the linear susceptibility (a, c, e), and group index (b, d, f) versus probe field wavelength for different energy splitting ω_s. The parameters are $p = 0.63$ and $\omega_s = 0.5\gamma$ (a, b), 9γ (c, d), 15γ (e, f). The other parameters are the same as Fig. 2

parameters (see Fig. 4). The results are in a good agreement with the obtained results for $p = 0.46$; increasing the energy splitting ω_s causes probe absorption to be decreased dramatically and simultaneously, the slope of dispersion changes from negative to positive. The reason can be explained as follows. By applying an increasingly intense tunneling through a thin barrier, the absorption for the probe field on the intersubband transitions $|1\rangle \to |3\rangle$ and $|1\rangle \to |2\rangle$ of the electronic medium can be reduced dramatically. This might be useful to control

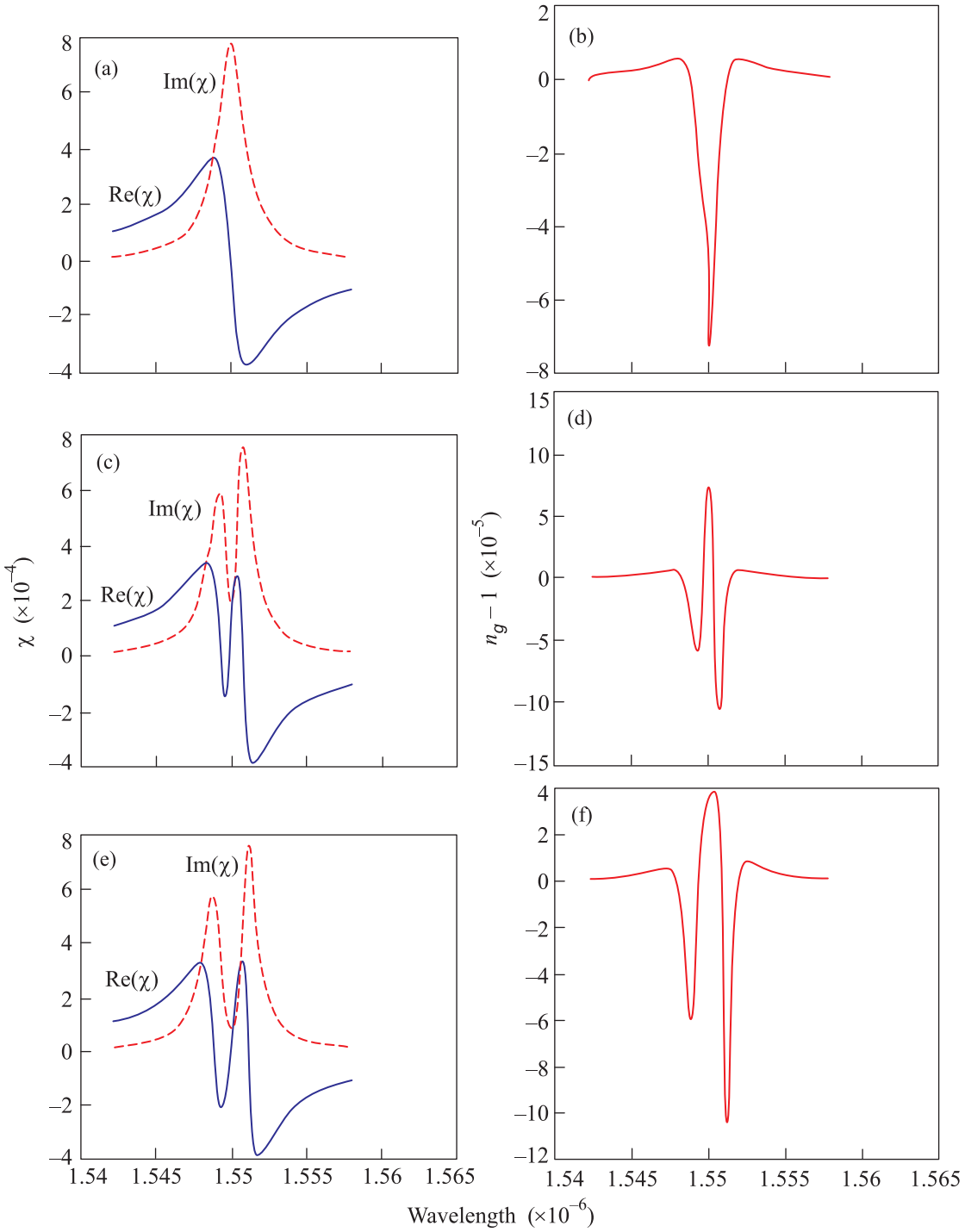

Fig. 5. Real and imaginary parts of the linear susceptibility (a, c, e), and group index (b, d, f) versus probe field wavelength for different energy splitting ω_s. The parameters are $p = 0.77$ and $\omega_s = 0.5\gamma$ (a, b), 9γ (c, d), 15γ (e, f). The other parameters are the same as Fig. 2

the probe absorption and dispersion simply by adjusting the splitting. The best curves to show the effect of energy splitting ω_s on linear susceptibility behavior of the electronic medium are displayed in Fig. 5. We observe the more reduction of absorption at long wavelength as we go from $\omega_s = 0.5\gamma$ to 15γ that is because of the impact of both the quality of Fano-interference ($p = 0.77$) as well as increasing the energy splitting ($\omega_s = 15\gamma$). In

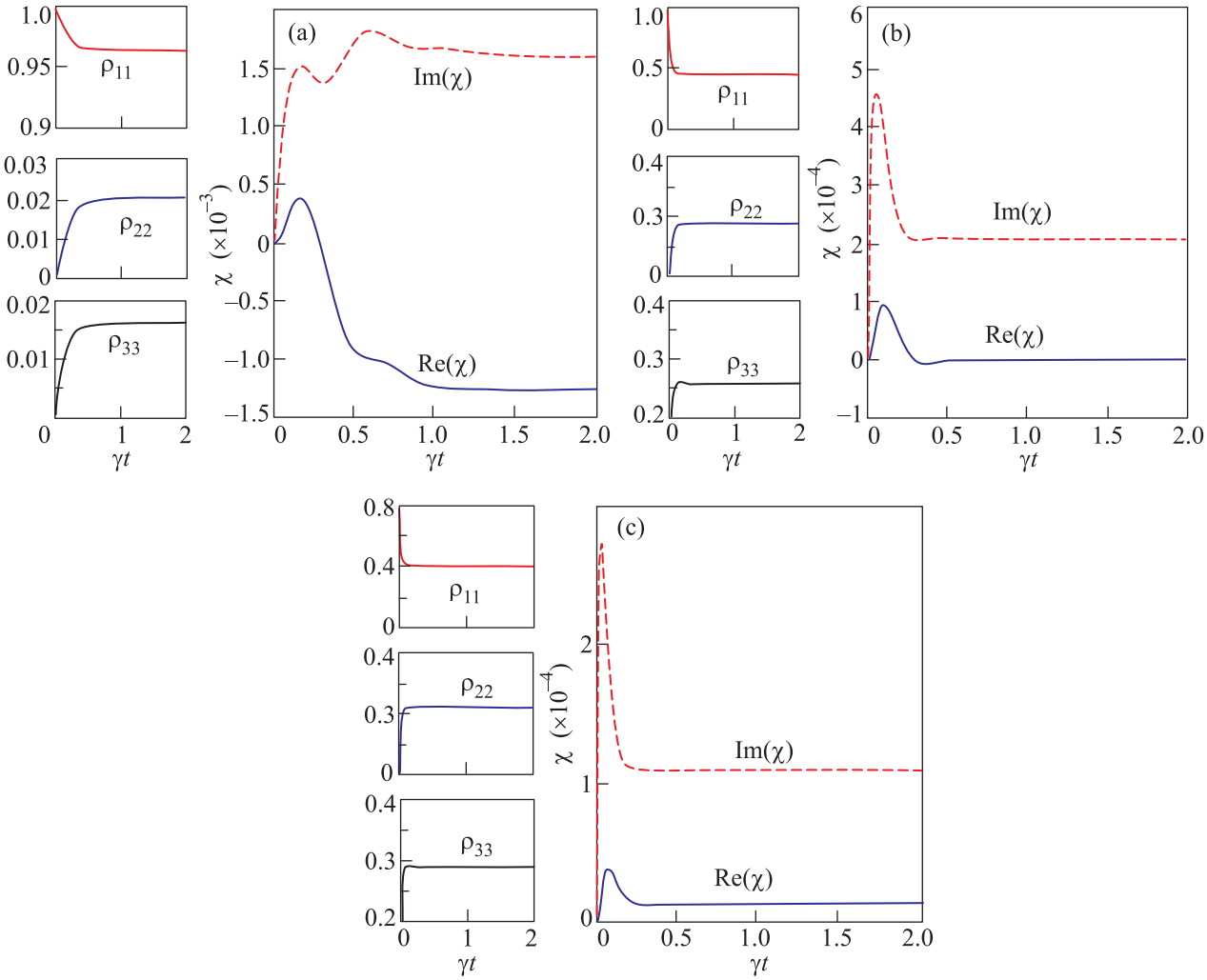

Fig. 6. Transient behaviors of probe field absorption and dispersion. Here, $p = 0.77$, $\lambda = 1550$ nm and the parameters values are $r = 0$ (a), 7.5γ (b), 15γ. The other parameters are the same as Fig. 2

this case, the transparency window will be appeared and the phenomenon is called EIT (Fig. 5e) [11]. Moreover, the slope of dispersion switches to positive which shows that light propagates in subluminal condition (Fig. 5f).

3.2. The case in presence of incoherent pumping; transient regime. Now, we are interested in the influence of incoherent pump fields and the quantum interference induced by incoherent pumping fields on transient optical properties of the medium. In order to study the effect of the incoherent pumping field on the quantum well system, two broadband polarized fields r_1 and r_2 ($r_1 = r_2 = r$) (can be provided by the diode laser that had a broad variable linewidth) that serve as the incoherent pumping fields and apply to the transitions $|1\rangle \to |2\rangle$ and $|1\rangle \to |3\rangle$, respectively (see Figs. 1c and d).

Thus, the Eq. (2) becomes as

$$\dot\rho_{12} = -\frac{\gamma_{21}}{2}\rho_{12} + i\left(\Delta_p - \frac{\omega_s}{2}\right)\rho_{12} - r\rho_{12} + i\Omega_{p_2}(\rho_{22} - \rho_{11}) + i\Omega_{p_1}\rho_{32} - \frac{\eta - \eta'}{2}\rho_{13},$$

$$\dot\rho_{13} = -\frac{\gamma_{31}}{2}\rho_{13} + i\left(\Delta_p + \frac{\omega_s}{2}\right)\rho_{13} - r\rho_{13} + i\Omega_{p_1}(\rho_{33} - \rho_{11}) + i\Omega_{p_2}\rho_{23} - \frac{\eta + \eta'}{2}\rho_{12},$$

$$\dot\rho_{23} = -\frac{\gamma_{32}}{2}\rho_{23} + i\omega_s\rho_{23} - r\rho_{23} + i\Omega_{p_2}\rho_{13} - i\Omega_{p_1}\rho_{21} - \frac{\eta - \eta'}{2}(\rho_{22} + \rho_{33}) + \eta'\rho_{11},$$

$$\dot\rho_{22} = -\gamma_2\rho_{22} + i\Omega_{p_2}(\rho_{12} - \rho_{21}) - \frac{\eta + \eta'}{2}(\rho_{23} + \rho_{32}) + r\rho_{11} - r\rho_{22},$$

$$\dot\rho_{33} = -\gamma_3\rho_{33} + i\Omega_{p_1}(\rho_{13} - \rho_{31}) - \frac{\eta + \eta'}{2}(\rho_{23} + \rho_{32}) + r\rho_{11} - r\rho_{33},$$

$$\rho_{11} + \rho_{22} + \rho_{11} = 1. \qquad (5)$$

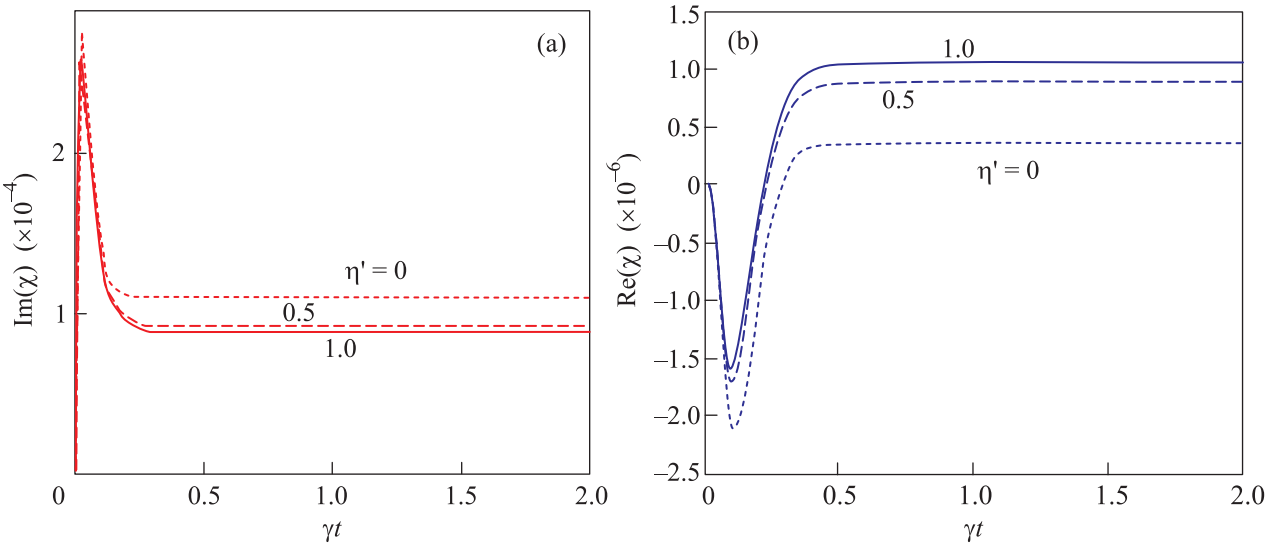

Fig. 7. Transient behaviors of probe field absorption (a) and dispersion (b) for different values of quantum interference arising from incoherent fields. Here, $p = 0.77$, $\lambda = 1550$ nm, $r = 15\gamma$ and the parameters values are the same as Fig. 2

The incoherent pump fields are added accordingly to the method described in Refs. [39–43]. The quantum interference induced by incoherent pumping fields is described by a parameter $\eta' \propto \sqrt{r_1 r_2}$, which is added following the Ref. [41]. In fact, if the polarizations of the two incoherent fields ε_1 and ε_2 properly be arranged in such a way that $\varepsilon_1\mu_{21} = \varepsilon_2\mu_{31} = 0$, thus one field acts on only one transition so that $\eta' = 0$ which means there is no interference due to incoherent pump fields. However, when $\varepsilon\mu_{21} \neq 0$ and $\varepsilon_2\mu_{31} \neq 0$, one polarized broadband field can couple with more than one transition, and thus $\eta' \neq 0$.

It is worth noting that the SQW sample used in this paper is very much similar to the one reported in reference [44] thus, we can keep the same parametric conditions here, and the three-level system of electronic subbands can be grown on the GaAs/AlGaAs substrate. Thus, the experimental feasibility of the scheme is evident.

Fig. 6 shows the transient evolution of the dispersion-absorption for various values of incoherent pumping field in QW system. In the following results we suppose the strong strength of Fano-interference, i.e., $p = 0.77$. We find out that the absorption-dispersion curves have an oscillatory behavior for a very short time and finally reach to the steady-state as time increases. In addition, it is obvious from Fig. 6a that in the absence of incoherent pumping ($r = 0$), the steady-state dispersion is negative corresponding to superluminal light propagation, which is accompanied with a large absorption. However, by increasing r to the larger values, the steady-state probe absorption reduce dramatically compared to the case $r = 0$. In addition, investigation on the dispersion curves (Figs. 6b and c), one can see that the steady-state probe dispersion becomes zero for $r = 7.5\gamma$, and then converts to positive for $r = 15\gamma$. Thus, increasing the rate of incoherent pumping results in subluminal propagation of light accompanied with reduced probe absorption. Physically, enhancing the rate of incoherent pumping field bring more population to the upper levels and thus, less population will remain in ground level $|1\rangle$, which can lead to reduction of the probe absorption. This condition is displayed in the left panels of Fig. 6. Obviously, as incoherent pumping increases, the population in lower level $|1\rangle$ reduces, while it is increased in both levels $|2\rangle$ and $|3\rangle$. In other words, increasing r makes the population difference between the lower and the upper levels to be larger. Thus, by applying an increasingly incoherent pumping field, one can decrease smoothly the absorption for the weak probe field and affect the absorptive-dispersive properties of the multiple QD molecules.

Finally, we are interested in the effect of the quantum interference arising from incoherent pumping fields η' on transient evolution of absorption and dispersion. In Fig. 7 we depicted the time evolution of the probe absorption-dispersion coefficients of the QW structure for $p = 0.77$ and $r = 15\gamma$. To have an estimate of the population contributed in probe absorption, the population distribution of the QW system is also presented in Fig. 8. It can be found that increasing the quantum interference parameter η' leads the steady-state probe absorption to be reduced dramatically (Fig. 7a). In ad-

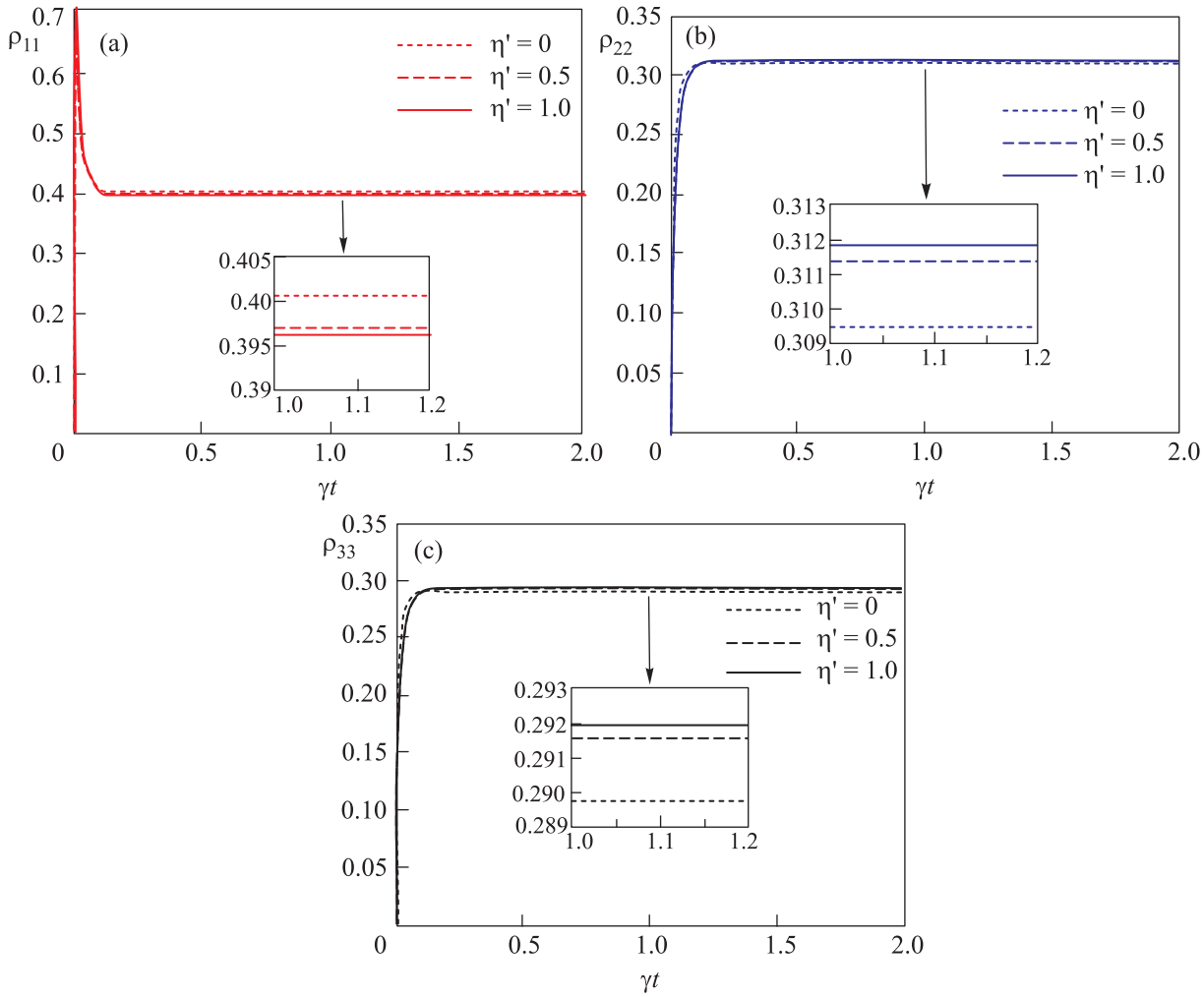

Fig. 8. Transient behaviors of population distribution ρ_{11} (a), ρ_{22} (b), and ρ_{33} (c) for different values of quantum interference arising from incoherent fields. The parameters values are the same as Fig. 7

dition, from Fig. 7b one can observe that the probe dispersion is very sensitive to the parameter η'. Obviously, by increasing the strength of quantum interference induced by incoherent pumping fields η', the steady-state probe dispersion finds higher positive values. For instance, for the perfect quantum interference $\eta' = 1$ (solid lines), the dispersion curve presents a much higher value corresponding to a much higher positive slope at long wavelength $\lambda = 1.55\,\mu$m that is accompanied with a reduced absorption. The reason for this behavior can be attributed to this point that more population will be trapped in upper levels for the strong quantum interference, which can be concluded from Fig. 8. So, the probe field absorption will be reduced. As one may know, the higher the slope of the positive dispersion is, the slower the propagating of light is. This is an important result which shows the extra controllability in this solid structure for the laser pulse to be slowed down at C-band Telecom wavelength.

4. Conclusion. In this paper, the transient and the steady-state properties of probe dispersion and absorption in a three-subband QW system is investigated. The effect of Fano-type interference as well as energy splitting of two excited states in light propagation is discussed. It is shown that by increasing the strength of Fano-interference the superluminal light propagation can be switched to subluminal light propagation which is accompanied with reduced probe absorption around long wavelength. In addition, dependence of probe absorption and dispersion on energy splitting is then discussed. It is shown that the group velocity of light pulse can be controlled with the rate of energy splitting. We also investigated the transient properties of the probe field affected with incoherent pump field. We found that

enhancing the rate of incoherent pumping transfer more population to the upper levels which leads to the reduction of probe absorption. Also, we showed that incoherent pumping has a major role in converting fast to slow propagation of light at C-band telecommunication $\lambda = 1550\,\text{nm}$ which is very practical in telecommunication science. Finally, an extra controllability is introduced for the light pulse to be more slowed down at Telecom wavelength band just through the quantum interference arising from incoherent pumping fields. It is worth noting that no external laser field is used at the pumping processes of the system. This advantage makes our electronic medium much more practical than its atomic counterpart that is because of its flexible design and the controllable interference strength.

The presented work has been supported by the Lithuanian Research Council (# VP1-3.1-ŠMM-01-V-03-001).

1. S. E. Harris, J. E. Field, and A. Kasapi, Phys. Rev. A **46**, R29 (1992); A. Kasapi, M. Jain, G. Y. Yin, and S. E. Harris, Phys. Rev. Lett. **74**, 2447 (1995).
2. O. Schmidt, R. Wynands, Z. Hussein, and D. Meschede, Phys. Rev. A **53**, R27 (1996); G. Muller, A. Wicht, R. Rinkleff, and K. Danzmann, Opt. Commun. **127**, 37 (1996).
3. J. E. Field, H. Hahn, and S. E. Harris, Phys. Rev. Lett. **67**, 3062 (1991); S. E. Harris, J. E. Field, and A. Imamoglu, Phys. Rev. Lett. **64**, 1107 (1990); S. E. Harris, Phys. Today **50**(7), 36 (1997).
4. M. Xiao, Y. Q. Li, S. Z. Jin, and J. Gea-Banacloche, Phys. Rev. Lett. **74**, 666 (1995); D. Budker, D. F. Kimball, S. M. Rochester, and V. V. Yashchuk, Phys. Rev. Lett. **83**, 1767 (1999).
5. L. G. Wang, N. H. Liu, and S. Y. Zhu, Phys. Rev. E **68**, 066606 (2003).
6. D. Han, H. Guo, Y. Bai, and H. Sun, Phys. Lett. A **334**, 243 (2005); C. Goren, A. D. Wilson-Gordon, M. Rosenbluh, and H. Fridmann, Phys. Rev. A **68**, 043818 (2003); G. S. Agarwal and T. Nath Dey, Phys. Lett. A **92**, 203901 (2004); H. Kang, L. Wen, and Y. Zhu, Phys. Rev. A **68**, 063806 (2003).
7. G. S. Agarwal, T. Nath Dey, and S. Menon, Phys. Rev. A **64**, 053809 (2001).
8. Zh. Duo, L. Jia-Hua, D. Chun-Ling, and Ya. Xiao-Xue, Commun. Theor. Phys. **59**, 594 (2013).
9. D. Zhang, Phys. Scr. **85**, 035401 (2012).
10. B. R. Mollow, Phys. Rev. A **5**, 2217 (1972).
11. K. Boller, A. Imamoglu, and S. E. Harris, Phys. Rev. Lett. **67**, 3062 (1991); S. E. Harris, J. E. Field, and A. Imamoglu, Phys. Rev. Lett. **64**, 1107 (1999); S. E. Harris, Phys. Today **50**(7), 36 (1997).
12. Y. Wu and X. Yang, Phys. Rev. A **71**, 053806 (2005).
13. Y. Wu, J. Saldana, and Y. Zhu, Phys. Rev. A **67**, 013811 (2003).
14. S. E. Harris and Y. Yamamoto, Phys. Rev. Lett. **81**, 3611 (1998).
15. M. Yan, E. G. Rickey, and Y. Zhu, Phys. Rev. A **64**, 041801 (2001).
16. H. Y. Ling, Y.-Q. Li, and M. Xiao, Phys. Rev. A **57**, 1338 (1998)
17. M. Sahrai, R. Nasehi, M. Memarzadeh, H. Hamedi, and J. B. Poursamad, Eur. Phys. J. D **65**, 571 (2011).
18. Zh. Wang, Physica E **43**, 1329 (2011).
19. Zh. Wang, Opt. Commun. **282**, 4745 (2009).
20. J.-H. Li, Opt. Commun. **274**, 366 (2007).
21. J.-H. Li, Phys. Rev. B **75**, 155329 (2007).
22. A. Imamog˘lu and R. J. Ram, Opt. Lett. **19**, 1744 (1994); H. Schmidt, K. L. Campman, A. C. Gossard, and A. Imamog˘lu, Appl. Phys. Lett. **70**, 3455 (1997).
23. J. Faist, F. Capasso, C. Sirtori, K. West, and L. N. Pfeiffer, Nature **390**, 589 (1997); M. D. Frogley, J. F. Dynes, M. Beck, J. Faist, and C. C. Phillips, Nature Mater. **5**, 175 (2006).
24. H. Schmidt, K. L. Campman, A. C. Gossard, and A. Imamo˘glu, Appl. Phys. Lett. **70**, 3455 (1997)
25. A. Joshi, Phys. Rev. B **79**, 115315 (2009).
26. A. Joshi and M. Xiao, Appl. Phys. B **79**, 65 (2004); J. H. Li and X. Yang, Eur. Phys. J. B **53**, 449 (2006); J. H. Li, Phys. Rev. B **75**, 155329 (2007).
27. Z. Wang, Opt. Commun. **282**, 4745 (2009); Z. Wang, H. Fan, and J. Lumin, **130**, 2084 (2010).
28. G. B. Serapiglia, E. Paspalakis, C. Sirtori, K. L. Vodopyanov, and C. C. Phillips, Phys. Rev. Lett. **84**, 1019 (2000); J. F. Dynes, M. D. Frogley, M. Beck, J. Faist, and C. C. Phillips, Phys. Rev. Lett. **94**, 157403 (2005).
29. G. B. Serapiglia, E. Paspalakis, C. Sirtori, K. L. Vodopyanov, and C. C. Phillips, Phys. Rev. Lett. **84**, 1019 (2000); J. F. Dynes, M. D. Frogley, M. Beck, J. Faist, and C. C. Phillips, Phys. Rev. Lett. **94**, 157403 (2005).
30. H. Schmidt and A. Imamo˘glu, Opt. Commun. **131**, 333 (1996).
31. J. H. Wu, J. Y. Gao, J. H. Xu, L. Silvestri, M. Artoni, G. C. La Rocca, and F. Bassani, Phys. Rev. Lett. **95**, 057401 (2005).
32. L. J. Wang, A. Kuzmich, and A. Dogariu, Nature **406**, 277 (2000).
33. O. Kocharovskaya, Y. Rostovtsev, and M. O. Scully, Phys. Rev. Lett. **86**, 628 (2001).
34. C. Liu, Z. Dutton, C. H. Behroozi, and L. V. Hau, Nature **409**, 490 (2001).
35. A. M. Akulshin, S. Barreiro, and A. Lezama, Phys. Rev. A **57**, 2996 (1998); A. Lezama, S. Barreiro, and A. M. Akulshin, Phys. Rev. A **59**, 4732 (1999).
36. A. V. Taichenachev, A. M. Tumaikin, and V. I. Yudin, Phys. Rev. A **61**, 011802 (2000).

37. H. S. Moon, S. K. Kim, K. Kim, C. H. Lee, and J. B. Kim, J. Phys. B: At. Mol. Opt. Phys. **36**, 3721 (2003).
38. C. Goren, A. D. Wilson-Grodon, A. Rosenbluh, and H. Friedmann, Phys. Rev. A **67**, 033807 (2003).
39. M. D. Lukin and A. Imamo˘glu, Phys. Rev. Lett. **84**, 1419 (2000).
40. Y. Zhu, Phys. Rev. A **55**, 4568 (1997).
41. W. H. Xu, J. H. Wu, and J. Y. Gao, J. Phys. B **39**, 1461 (2006).
42. H. F. Zhang, J. H. Wu, X. M. Su, and J. Y. Gao, Phys. Rev. A **66**, 053816 (2002).
43. X. M. Su, H. X. Kang, J. Kou, X. Z. Guo, and J. Y. Gao, Phys. Rev. A **80**, 023805 (2009).
44. A. Imamog˘lu and R. J. Ram, Opt. Lett. **19**, 1744 (1994).